NANOSYSTEMS: PHYSICS, CHEMISTRY, MATHEMATICS, 2020, 11 (4), P. 391–400

Effect of doping concentration on optical and electrical properties of intrinsic n-type ZnO (i-ZnO) and (Cu, Na and K) doped p-type ZnO thin films grown by chemical bath deposition method

Vipul Shukla[1], Dr. Amit Patel[2]

[1]Gujarat Technological University, Ahmedabad – 382424 Gujarat, India
[2]Government Engineering College, Godhra – 389001 Gujarat, India

vipuljshukla317@gmail.com

DOI 10.17586/2220-8054-2020-11-4-391-400

Pure ZnO and copper (IB group), sodium (IA group) and potassium (IA group) and doped ZnO thin films on glass substrate by chemical bath deposition method have been studied for Hall effect measurements, resistivity, Raman and photoluminescence (PL). The influence of dopant content on carrier concentration, electrical resistivity, and Hall mobility of the thin films are analyzed. Electrical conductivity measurements of ZnO are carried out by two probe method and activation energy for the electrical conductivity of pure and doped ZnO is found out. The Raman scattering of the pure ZnO and doped ZnO shows the first and second orders of polar and non-polar modes. Raman spectra confirms the hexagonal wurtzite structure of pure and doped ZnO with E_2 (high) mode at 439 cm^{-1} and presence of other possible defects. Photoluminescence (PL) at room temperature results indicate the emission occurs at close band lines and the outcomes are identified with a few inherent imperfections in the doped ZnO thin films. The PL results demonstrate the upgraded optoelectronic properties, specifically, the carriers for long life span is executed by the oxygen opportunities. Raman spectroscopy and photoluminescence confirm existence of zinc interstitials (Zni) as well as oxygen vacancies (Vo). Resistivity as low as 15 Ω-cm, Hall mobility as high as 6.2 cm^2/Vs and effective carrier concentration as high as $1.70\times10^{17} e^-/cm^3$ have been obtained.

Keywords: Raman spectroscopy, photoluminescence spectroscopy, electrical properties, pure and doped ZnO, thin films.

Received: 14 April 2020

Revised: 11 July 2020

1. Introduction

Zinc oxide (ZnO) with its one of a kind physical and synthetic properties e.g. high chemical stability and high electrochemical coupling coefficient, wide scope of radiation absorption and high photostability, is a multifunctional material [1,2]. ZnO is an n-type semiconductor, its electrical conductivity is mainly due to excess zinc at interstitial positions. ZnO works as a potential applicant for the optoelectronics, photonics, piezoelectric and solar cell applications because of its specific band gap (3.37 eV) and expansive exciton binding energy (60 meV) at room temperature [3,4]. ZnO exhibits greatest variety of nanostructures. ZnO is the key material for various potential applications such as photodetectors, laser diode, sensors,flexible and polymer based solar cells and an electrode in dye sensitized solar cells. Many research groups are working for the development of ZnO nanostructures based white light emitting diode (LED) as an alternative source to enable bright and energy saving light sources [5–7]. Electrical properties of ZnO thin films doped with materials like Cu are very useful for optoelectronic applications [8] however efficiency of such films found limited due to formation of donor compensating point defects [9]. Coulomb interactions between dopant and acceptor-like defects, such as oxygen interstitial lead to bound complexes [10, 11]. The combination of p-type and n-type material reduces the recombination rate of photo generated electrons and holes [12].

We performed methodical Raman spectroscopy studies to examine the vibrational symmetry qualities of the pure doped ZnO films. Progress in metal doped ZnO works are effectively encouraging possibility for spintronics and photonics applications because of their one of a kind properties [13, 14]. Raman spectra indicated a successful incorporation of K ions into the ZnO lattice [15]. Moreover, the Raman spectroscopy is a versatile technique to study the doping agent incorporation and impurity induced modes of ZnO nanoparticles doped with metals [16]. By introducing various ions in the crystal lattice of ZnO, its optical properties can be modified [17].

PL emission spectroscopy is a traditional technique to determine optical properties and internal defects of metal doped ZnO nanostructures [18]. ZnO is an n-type semiconductor. ZnO is expected to be p-doped by elements of IA group (such Li, Na, and K), IB group (such as Cu, Ag, Au), or V–A group (such as N, P, As, Sb) [19]. Electrical properties of ZnO vary significantly due to carrier concentration, mobility and resistivity. The Hall effect is the most extensively used method to measure the electrical properties. Resistivity and Hall Measurements were made by the van der Pauw method [20, 21] to study the conductivity phenomena across square-shaped samples. Doping of various impurity elements in ZnO shows different functions and improved properties of semiconductor compounds

such as electrical, optical and mechanical, which facilitate the development of many electronic and optoelectronic devices [22–24].

Many investigations are carried out to improve the characteristics of ZnO thin films by doping in it with various materials. However, investigations of Cu, Na and K doped ZnO thin films are very scarce, also,to the best of our knowledge, there is no study which compares the effects of these dopants on electrical and optical properties of ZnO. Moreover, most studies are concentrated around the ZnO thin films developed by physical routes and little research has been done on the same developed by chemical route. Thus, it is of interest to us to investigate the influence of the Cu, Na and K dopant elements on the properties of ZnO thin films deposited by chemical routes. Therefore, we set out an easy, well-grounded and low-cost method for growing and doping ZnO with Cu, K and Na dopant using Chemical Bath Deposition, in aqueous solution. Influence of doping on electrical and optical parameters like resistivity, conductivity, mobility, carrier concentration, band gap values and ionization energies of impurity levels were investigated.

2. Experimental details

Pure ZnO thin films were synthesized by chemical bath deposition method following the same procedure as reported earlier [25]. Aqueous solutions of 0.1 M 20 ml copper chloride, 0.1 M 20 ml sodium chloride and 0.1 M 20 ml potassium chloride were added to 0.1 M 60 ml zinc chloride solution for the growth of copper doped ZnO (Cu:ZnO), sodium doped ZnO (Na:ZnO) and potassium doped ZnO (K:ZnO) respectively. After that it was mixed with aqueous ammonia solution.

3. Measuring instruments

Reni shaw in Via Raman Microscope with a laser excitation source ($\lambda = 514$ nm) was used to record Raman scattering spectra at room temperature. PL (photoluminescence) spectrum of all the samples were recorded at room temperature using a Shimadzu RF-5301 PC spectro-fluoro- photometer under an excitation wavelength of $\lambda = 325$ nm and the emission spectra was recorded at the wavelength range of 350 – 550 nm. Ozone free Xenon-quartz lamp of 150 W was used for excitation. Hall-effect measurements were carried out in the van der Pauw configuration (DNE 21A) at room temperature for the determination of type of conduction mechanism, Hall mobility and carrier concentration. Electrical conductivity and activation energy were determined by the two probe resistivity measurement performed on all the samples from room temperature to 200 °C.

4. Result and discussion

4.1. Raman spectroscopy

In order to determine the presence of dopant-resulted defects and deficiency in lattice of source crystal,especially with regards to material separate on or second level states in material, Raman spectroscopy is used as an adaptable technique. The vibrational properties of all the four films are investigated by Raman spectra. ZnO thin films with hexagonal wurtzite structure fit into the P63mc position group. The first-class Raman scattering involves only the optical phonons at Γ point of the Brillouin zone for the ideal ZnO crystal lattice. As per the group theory, wurtzite ZnO should be with optical modes and they can be formulated by the following equation:

$$\Gamma_{\mathrm{opt}} = 1\mathrm{A}_1 + 2\mathrm{B}_1 + 1\mathrm{E}_1 + 2\mathrm{E}_2,$$

where, two polar branches A_1 and E_1 modes split into longitudinal optical (LO) and transversal optical (TO) segments having difference in their frequencies, as macroscopic electric fields are related with the LO type phonons. As a First order Raman-active modes, the A_1, E_1 and E_2 modes are considered. In order to investigate the effect of doping of Cu, Na and K on host ZnO vibrational properties are investigated for pure as well as doped thin films. Raman spectra for pure ZnO, Cu: ZnO, Na: ZnO and K: ZnO are shown in Fig. 1 and results are summarized. At 138, 338, 439 and 605 cm^{-1}, peaks representing E_{2L}, $2\mathrm{E}_{MO}$, E_{2H} and A_{1LO} respectively, the fundamental modes of hexagonal ZnO are observed. Polar mode A_1 (LO) at around 605 cm^{-1} is also found present in all doped samples. This peak is shifted to lower energy. All the shifting and broadening of phonon modes represent the scattering contributions outside the Brillouin zone center. A_1 (LO) mode of phonon is usually referred to the complexes having zinc interstitial defect and vacancy created by oxygen in ZnO lattice. The defect complexes of zinc interstitial and oxygen vacancy in ZnO lattice can represent using a A_1 (LO) type mode of phonon [26]. These interstitial incorporation of Cu, Na and K might have caused significant structural disorder in ZnO, producing the observed changes in the line width and position of the Raman peaks.

Raman spectra presented in Fig. 1 show several peaks at 138, 338, 439, 605 and 1123 cm^{-1} correspond to E_2 (low), E_2 (high) – E_2 (low), E_2 (high), A_1 (LO) and 2(LO) vibration modes respectively. The peak at 338 cm^{-1} was attributed to second order phonon method because of multiple phonon processes [27]. E_2 (high) mode of pure

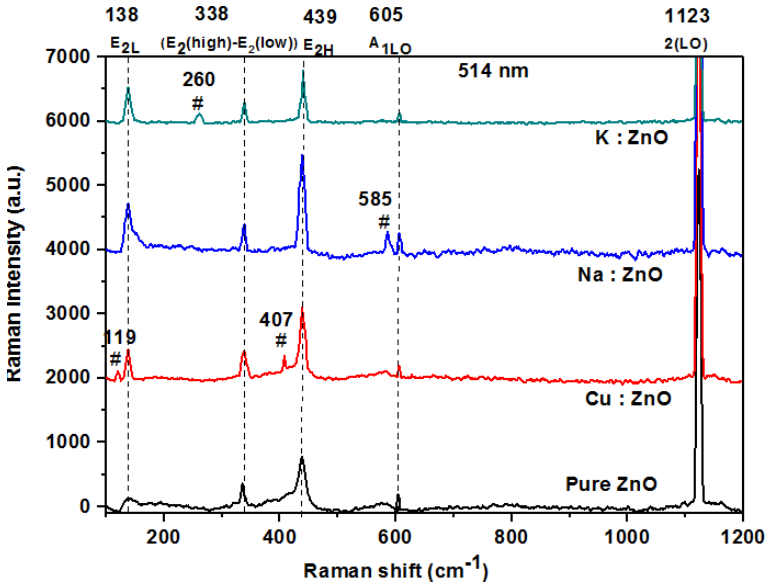

FIG. 1. Raman spectra of undoped and doped ZnO films grown on glass. The background has been removed, and the spectra have been vertically offset for clarity

and doped ZnO can be attributed to the good crystallinity of the films and this mode indicates the band characteristic of wurtzite-structured ZnO [28]. The A_1 (LO) (605 cm^{-1}) and 2LO (1123 cm^{-1}, which is normally inactive in the infrared) are respectively the first and second order of the LO phonons at the Γ center of the Brillouin zone. These vibrations were shown to present a resonant profile and are attributed to localized excitations that are strongly coupled to the lattice through the Fröhlich interactions [29].

Finally, we point out that some of the additional peaks appear in the spectra of ZnO thin films with certain dopant species, indicating host lattice defects in the ZnO structure only, which is shown with "#" such as the peak at 119 and 407 cm^{-1} for the Cu doped, at 585 cm^{-1} for the Na doped, and at 260 cm^{-1} for K doped thin films. These modes seem to be related to the individual dopants, and may be used as indication for their incorporation.

4.2. Photoluminescence studies

Effect of doping on the optical properties was also investigated by photoluminescence (PL) spectra of all the four thin films at room temperature. Emission PL spectra with excitation wavelength of 325 nm has been recorded.

There are two parts in the emission spectrum of ZnO thin film: Excitonic near band edge (NBE) emission in the UV region, with energy approximately the band gap of ZnO and the deep level emission (DLE) in the visible region arising from intrinsic defects as well as extrinsic impurities. The DLE shows numerous peaks subjected to the nature of intrinsic defects, their complexes and extrinsic impurities. The concentration of these defects and impurities transform the pattern and status of peaks in terms of position.

TABLE 1. PL peak position of pure and doped samples

Thin Film	Peak position at wavelength $\lambda_{ex} = 325$ nm		
	NBE (Near band edge emission) Violet emission	DLE (Deep level emission) Blue emission	DLE (Deep level emission) Green emission
Pure ZnO	380 nm (3.27 eV)	484 nm (2.56 eV)	534 nm (2.32 eV)
Cu:ZnO	386 nm (3.21 eV)	—	520 nm (2.38eV)
Na:ZnO	397 nm (3.12 eV)	—	—
K:ZnO	392 nm (3.16 eV)	486 nm (2.55 eV)	—

In the present study the PL peak at 380, 386, 397 and 392 nm correspond to photon energy 3.27, 3.21, 3.12 and 3.16 eV for pure ZnO, Cu:ZnO, Na:ZnO and K:ZnO respectively are smaller than band gap of the ZnO at room

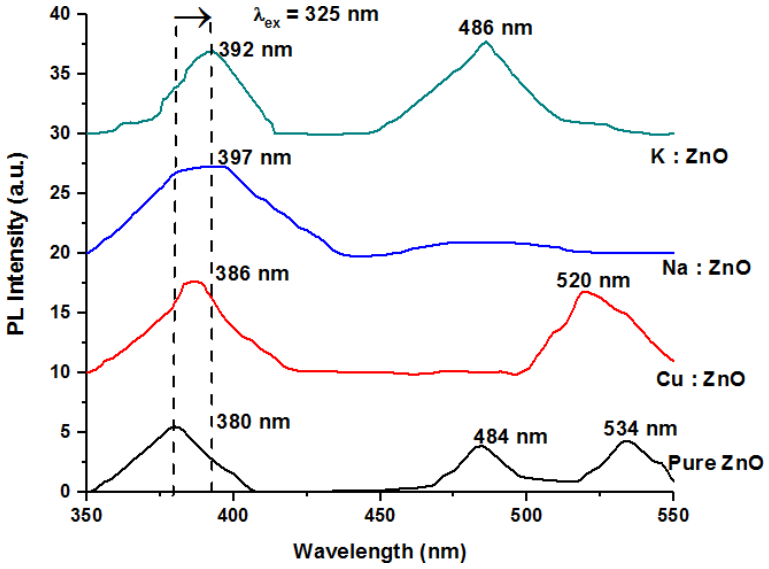

FIG. 2. Red-shift of the UV peaks in PL spectra for the Cu-, Na- and K- doped ZnO compared to the undoped ZnO thin films

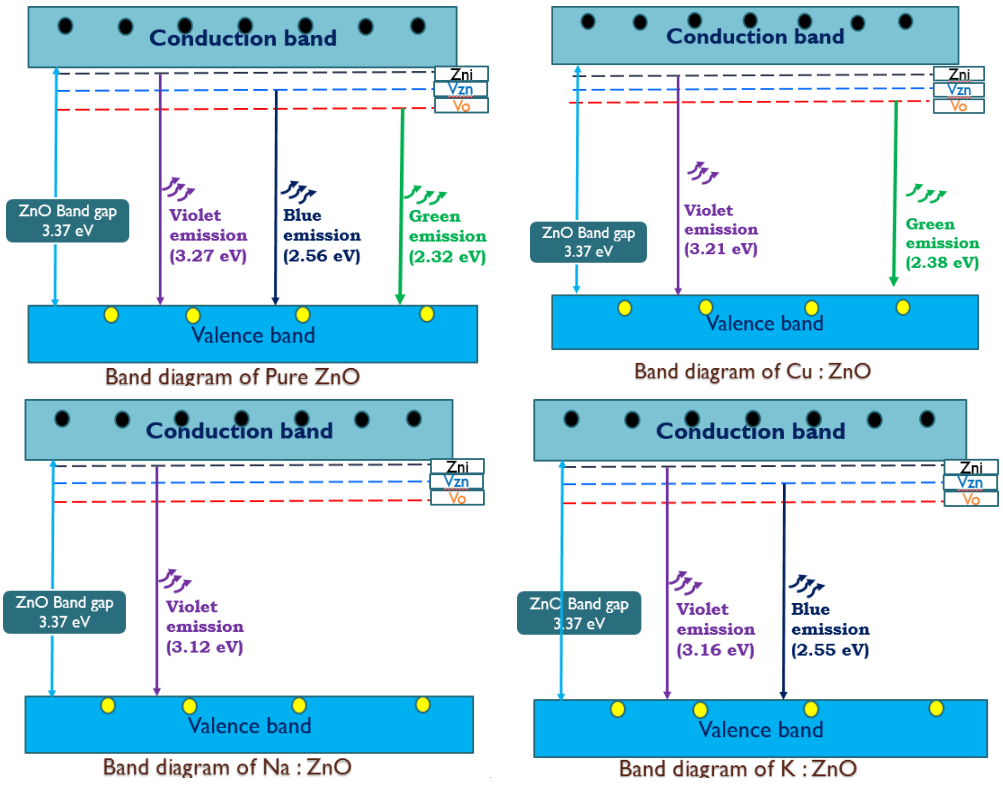

FIG. 3. Band diagram of Pure ZnO and Cu, Na and K doped ZnO thin films

temperature (3.37 eV), which is not due to the band-band transition between valence band and conduction band but it's a near band emission (NBE), which are due to the recombination of free excitons. The deep level emission (DLE) peaks recorded at 484 – 486 nm are mainly due to oxygen vacancies (Vo) in the compounds and zinc interstitials [30]. The green band at 534 and 520 nm for pure ZnO and Cu doped ZnO thin films are mainly due to the oxygen related effects like zinc interstitials (Zni), oxygen vacancies (Vo) and antisite oxygen (Ozn). The violet emission presumably resulted from a close relation with defects such as interstitial Zn atoms (Zni) and ions in the ZnO lattice.

In the case of pure ZnO, oxygen vacancies play an important role in the origin of green peak at ∼534 nm. However, the precise mechanism of green emission in ZnO is not yet assured and energy levels of various defects stated in literature differ greatly. Moreover,several reports hint that the green emission in ZnO is a result of oxygen vacancies and Cu impurities. Dingle pointed that the charge transfer from impurity states (Cu^{2+}) to concerned valence band is positively factor of green lumine scence in Cu–ZnO [31]. In addition to this model as suggested by Garces et al. [32], Cu may be either in Cu^{+} or Cu^{2+} state. It is referred that monovalent state (Cu^{+}) will contribute structure with less emission as a result of donor–acceptor pair recombination in which shift from the copper acceptor to superficial donor impurity happens. In the present research, green luminescence in undoped ZnO, may be caused by the presence of constitutional defects in ZnO. Moreover, there is slight possibility of oxygen vacancy, which is also an explanation of green emission in pure ZnO. However, a fair intensification in green emission in Cu: ZnO samples points out the contribution of Cu in green emission. It also recommends that the improved green emission is predominantly owing to copper-impurities. Thus, enhancement in n-type conductivity (Table 2) and appearance of green emission after copper doping in ZnO supports that the Cu is doped in ZnO lattice that is the cause of green emission. CuO film is an effective absorbing layer in the field of solar energy [33].

TABLE 2. Optical and electrical data of Pure ZnO and Cu, Na and K doped ZnO thin films deposited on glass substrate with various doping concentrations

Sample	Resistivity ρ (Ω cm)	Conductivity σ (S/cm)	Mobility μ (cm^2/Vs)	Hall coefficient R_H (cm^3/C)	Carrier concentration n (e^-/cm^3)	Activation Energy E_a (eV)
Pure ZnO	72.14	0.0139	0.525	37.84	1.651×10^{17}	0.038
0.1M Cu:ZnO	78.57	0.0127	0.603	47.40	1.318×10^{17}	0.034
0.2M Cu:ZnO	59.29	0.0169	0.744	44.10	1.418×10^{17}	0.033
0.3M Cu:ZnO	45.00	0.0222	0.876	39.40	1.585×10^{17}	0.029
0.4M Cu:ZnO	35.71	0.0280	1.064	38.00	1.644×10^{17}	0.027
0.5M Cu:ZnO	15.00	0.0667	2.447	36.70	1.703×10^{17}	0.027
0.1M Na:ZnO	72.14	0.0139	5.877	424.00	1.473×10^{16}	0.057
0.2M Na:ZnO	67.86	0.0147	4.509	306.00	2.043×10^{16}	0.057
0.3M Na:ZnO	60.71	0.0165	3.047	185.00	3.375×10^{16}	0.047
0.4M Na:ZnO	43.57	0.0230	1.985	86.50	7.227×10^{16}	0.035
0.5M Na:ZnO	22.86	0.0438	3.588	82.00	7.620×10^{16}	0.033
0.1M K:ZnO	78.57	0.0127	2.456	193.00	3.236×10^{16}	0.048
0.2M K:ZnO	70.00	0.0143	2.557	179.00	3.498×10^{16}	0.045
0.3M K:ZnO	56.43	0.0177	2.446	138.00	4.531×10^{16}	0.017
0.4M K:ZnO	35.00	0.0286	3.714	130.00	4.792×10^{16}	0.023
0.5M K:ZnO	20.00	0.0500	6.200	124.00	5.033×10^{16}	0.020

The red-shift in UV emission is observed in PL spectra of doped ZnO. This red-shift in the UV emission could be an outcome to get p-type ZnO. A widening of the band-gap indicated ZnO doping with donors; while p-type ZnO has indicated reduced band-gap whenever doped with acceptors.

4.3. Electrical measurements

4.3.1. Resistivity measurements. Temperature dependence of electrical resistivity of pure and doped ZnO thin films with different dopant concentrations was measured by two probe resistivity measurement method from room temperature to 200 °C. The resistivity (ρ) of the samples was calculated by using the formula:

$$\rho = \frac{RA}{l},$$

where R is the resistance, A is the cross sectional area and l is the length of a thin film.

Resistivity of a 0.1 M Pure ZnO is 72.14 Ω·cm but by increasing the precursor concentration from 0.1 to 0.5 M of Cu, Na and K doped ZnO, the resistivity value decreases as shown in Table 2. The decrease in resistivity of Cu, Na and K doped ZnO thin films with concentration might be due to the capture of free electrons in ZnO lattice by the empty lower energy 3d Cu states.

The electrical conductivity of the Cu:ZnO, Na:ZnO and K:ZnO films depended on the oxygen vacancies and the contribution from the Zn–Cu, Zn–Na and Zn–K interstitial atoms. The resistivity of the Cu:ZnO, Na:ZnO and K:ZnO films decreased from 78.57 to 15 Ωcm, 72.14 to 22.86 Ωcm and 78.57 to 20Ωcm as the doping concentration increased from 0.1 M to 0.5 M respectively. The conductivity was increased because of the reduction in the grain-boundary scattering. The carrier concentration of pure ZnO is 1.651×10^{17}e$^-$/cm^3 and for Cu: ZnO, Na: ZnO and K:ZnO films is increased from 1.318×10^{17} to 1.703×10^{17}e$^-$/cm^3, 1.473×10^{16} to 7.620×10^{16}e$^-$/cm^3 and 3.236×10^{16} to 5.033×10^{16}e$^-$/cm^3 as the doping concentration increased from 0.1 M to 0.5 M respectively. Mobility of the pure ZnO film was found to be 0.525 cm^2/Vs, by adding impurity like Cu and K mobility is increased from 0.60 to 2.45 cm^2/Vs and 2.46 to 6.2 cm^2/Vs but for Na doped it decreases from 5.88 to 3.59 cm^2/Vs as the doping concentration increased from 0.1 M to 0.5 M respectively which showed improvements in the properties of the doped thin films (Table-2).

4.3.2. Activation energy. The energy required to shift charge from one primarily neutral species to another is called as activation energy and written by E_a. This is identical to the electrostatic binding energy of the charge to the species. When these charge carriers are being excited to at least activation energy from the Fermi-level, there will be channeling from one species to another. These species or small particles are called crystals. The activation energy is associated with film conductivity [31] and correlated by this formula:

$$\sigma = \sigma_0 e^{-[E_a/2k_BT]},$$

where, σ_0 is the conductivity at 0 °C and k_B is the Boltzmann constant and T is the absolute temperature. The equation can be written as:

$$\ln\sigma = \frac{-E_a}{2k_BT} + \ln\sigma_0.$$

This equation is equivalent to a straight line equation, $y = mx + c$. So that can be determined from the slope of the straight line. From the graph of $\ln\sigma$ Vs $1/T$, can be calculated by using the relation:

$$E_a = \left(\frac{-\ln\sigma}{1/T}\right) \times 2k_B \ \text{(eV)}.$$

The activation energy represents the location of trap levels below the conduction band. In the present study activation energies of the undoped and Cu, Na and K doped ZnO films were studied and recorded in Table 2. The activation energy can be extracted from the slopes of the fitting lines. Fig. 4 shows the variation of $\log\rho$ with reciprocal of temperature for the Cu, Na and K doped ZnO thin film. It is observed that resistance increases with increasing temperature indicating semiconducting nature of the films. From the slopes of $\log\rho$ Vs $1000/T$ plots the values of activation energies (Table 2) were calculated using the formula:

$$\text{Activation energy } E_a = 2.303 \times k_B \times 10^3 \times \left(\frac{-E_a}{R}\right) \ \text{(eV)},$$

where $k_B = 8.602 \times 10^{-5}$ eV/K.

4.3.3. Measurements of Hall parameters. Hall measurements have been carried out at room temperature. In order to obtain p-type of ZnO it is necessary provide the compensation of native donor defects such as oxygen vacancies and interstitial zinc atoms by doping. The defects in hydrogen interstitial and oxygen vacancy and the addition of the Cu, Na and K dopant produced carriers in the films. Usually the concentration of these defects in ZnO is very large. Thus, that demands very high concentration of acceptors. P-type ZnO is difficult to obtain due to their low solubility in ZnO, wide band gap and low valence band energy. The self-compensation from donors and high ionization energy of acceptors are the two main problems hindering the enhancement of free hole concentration. Current limitations to p-doping limit electronic and optoelectronic applications of ZnO, which usually require junctions of n-type and

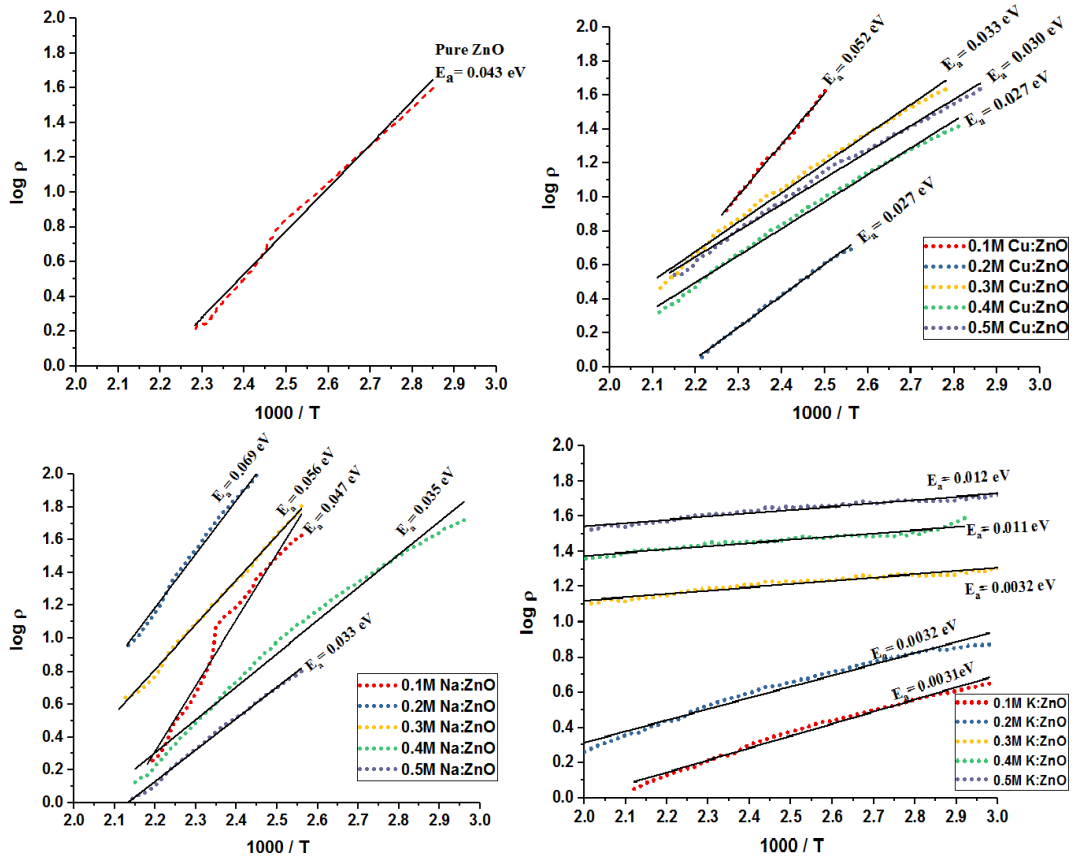

FIG. 4. Curve between $\log \rho$ and $1000/T$ of pure and doped ZnO thin films

p-type material. Known p-type dopants include group-I elements Li, Na, K; group-V elements N, P and As; as well as copper and silver. However, many of these form deep acceptors and p-type conduction is not significant at room temperature [1].

The Hall effect study is to compute the type of carriers. The activation energy relies on the donor carrier concentration and energy levels of the impurity. An increment in donor carrier concentration brings the Fermi level up in the energy gap and results in the reduction of activation energy [34].

Hall effect measurements had conducted on a sample grown on glass substrate as the magnetic field diverse from 0.1 to 1.5T. Hall effect measurement is conducted for the sixteen thin films, one film of 0.1 M pure ZnO and five films of Cu, K and Na doped ZnO each, for the variation of doping concentration from 0.1 to 0.5 M.The Hall coefficient is defined as:

$$R_H = \frac{V_H \times t}{I \times B},$$

where R_H is Hall coefficient, V_H is Hall voltage, t is the thickness of the film, I is the current passing through the conductor and B is the magnetic field. The Hall coefficient reveals the nature of the charge carriers, their concentration in the conductor, and their charge. The formula of carrier concentration (n) and mobility (μ) are:

$$R_H = \frac{-1}{n \times q},$$

$$\mu = \frac{R_H}{\rho},$$

where n is the concentration of the carriers, q is the charge of a single carrier.

Figure 5 shows the variation in the different electrical transport parameters such as the resistivity (ρ), the Hall coefficient (R_H), the carrier (electron–hole) concentration (n) and the mobility (μ) for the variation in doping concentration of the doped thin films. It is conclude that in all samples, resistivity and ionization energy decreases with increasing doping concentration. Also carrier concentration increases with doping concentration. The graph of mobility Vs doping concentration, mobility seems to be increasing with doping concentration in all samples for Cu and

K doping but for Na doping mobility decreases for 0.3 M concentration then it is increases as precursor concentration increases. Also the rate of the increment is very low in copper-doped ZnO thin films. The negative value of the Hall coefficient (R_H) for the pure ZnO film indicates its n-type conducting nature whereas; thepositive values of R_H for all of the doped ZnO films signify their p-type conductivity. The carrier (electron) concentration for the undoped ZnO is found to be 1.651×10^{17}cm^3. On the other hand, both the carrier (hole) concentration and the carrier mobility in all doped ZnO films are found to increase gradually as we change the doping concentration from 0.1 to 0.5 M. The p-type conductivity mainly arises due to the doping of the alkali metals in ZnO. The doped films do not contain a significant amount of Vo which acts as a donor within the ZnO films.The substitution of monovalent alkali ions (Na^+ and K^+) at the Zn^{2+} ion sites can introduce holes into the system [35, 36].

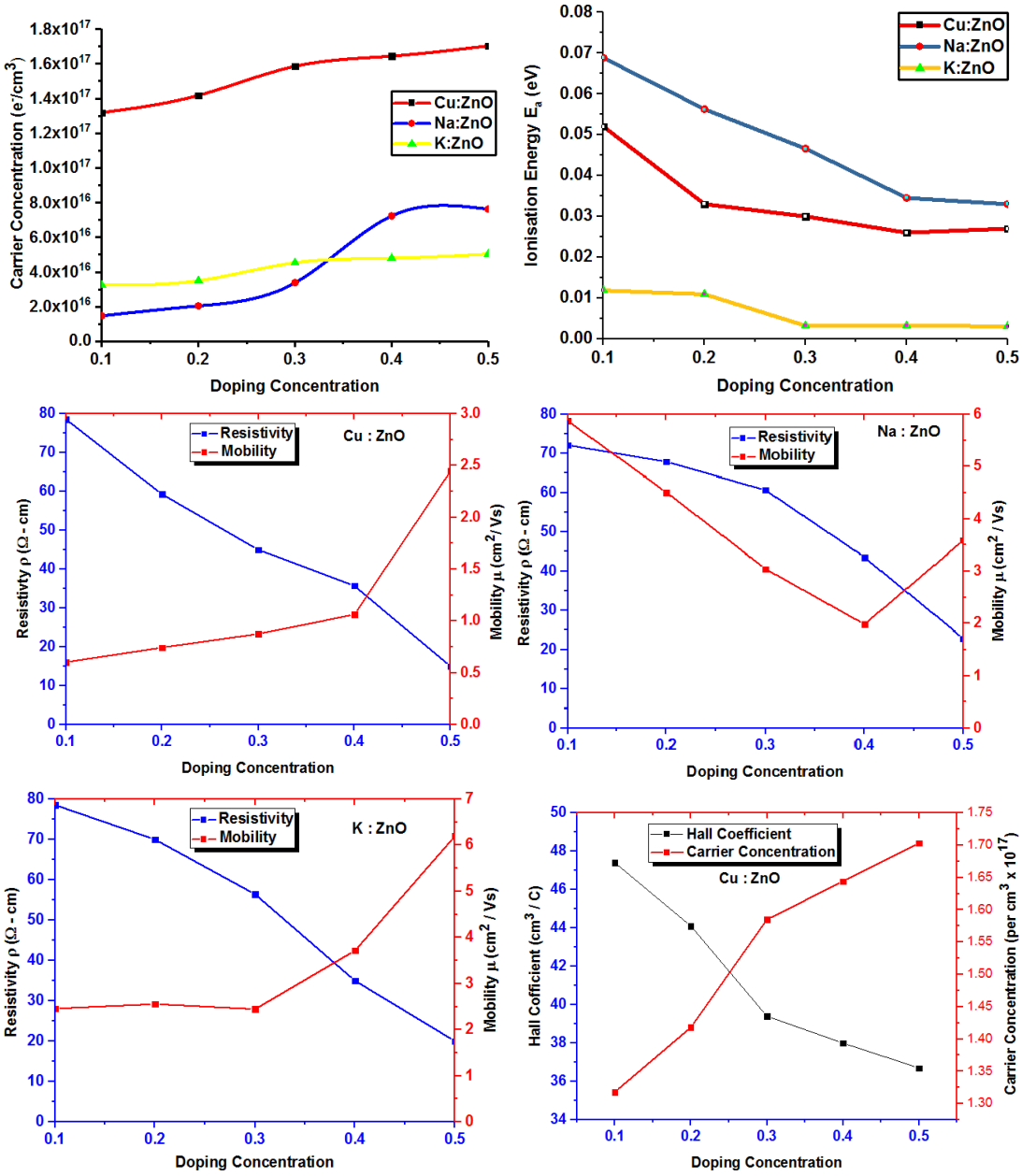

FIG. 5. Shows variation in resistivity (ρ), carrier concentration (n), mobility (μ) and ionization energy (E_a) of a Cu, Na and K doped ZnO thin films with variation in doping concentration from 0.1 to 0.5 M

5. Conclusion

In summary, complete and careful comparison of pure ZnO and copper (Cu), potassium (K) and sodium (Na) doped ZnO thin films has been carried out. All three dopants improve film optical and electrical properties compared to undoped ZnO. The Raman spectra show that the intensity of the dominant peak changes with different dopant; compared to the ZnO thin film, the shifting of peaks is due to lattice defects and lattice disorder. Decrease in band gap supports optical properties of crystalline structures. Green deep-level emission obtained in PL is potentially important for solar cell devices. The synchronous Raman and photoluminescence examinations have the preferred standpoint to correspond with the changes observed in the optical property of the semiconducting materials. Hall effect results show that a growth condition is suitable for p-type doped ZnO thin films with high carrier concentration. Also, chemical bath deposition method to grow doped ZnO increases stability of p-type ZnO. The positive value of Hall voltage of all doped thin films measured using Van der Pauw method with four point electrode fixture is in agreement with the red shift in PL spectra of p-type doping. The decrease in resistivity of all three doped thin films compared with ZnO films is attributed to the replacement of Zn^{2+} by Cu^{2+}, Na^{+} and K^{+} ions respectively. The resistivity of all doped thin films decrease with increase in doping concentration. As the concentration of impurity increases, both the conductivity and mobility of thin films increase. Activation energy has been observed to decrease with an increase in dopant concentration as well as change in dopant. ZnO thin films doped with Cu, Na and K has the capability to increase its conductivity without adversely modifying other properties. The deposited films find suitable for photocells and solar cell gadgets.

References

[1] Segets D., Gradl J., et al. Analysis of optical absorbance spectra for the determination of ZnO nanoparticle size distribution, solubility, and surface energy. *ACS Nano*, 2009, **3**, P. 1703–1710.

[2] Lou X. Development of ZnO series ceramic semiconductor gas sensors. *J. Sens. Trans. Technol.*, 1991, **3**, P. 1–5.

[3] Wang J.X., et al. Free-standing ZnO–CuO composite nanowire array films and their gas sensing properties. *Nanotechnology*, 2011, **22** (32), P. 1–7.

[4] Janotti A., Van De Walle C.G. Fundamentals of zinc oxide as a semiconductor. *Reports Prog. Phys.*, 2009. **72** (126501), P. 14–29.

[5] Wang Z.L. Zinc oxide nanostructures: growth, properties and applications. *J. Phys. Condens. Matter*, 2004, **16**, P. R829–R858.

[6] Gomez J.L., Tigli O. Zinc oxide nanostructures: From growth to application. *Journal of Materials Science*, 2013, **48** (2), P. 612–624.

[7] Schmidt-Mende L., Macmanus-Driscoll J.L. ZnO: nanostructures, defects, and devices. *Materials Today*, 2007, **10** (5), P. 40–48.

[8] Rana V.S., Rajput J.K., Pathak T.K., Purohit L.P. Cu sputtered Cu/ZnO Schottky diodes on fluorine doped tin oxide substrate for optoelectronic applications. *Thin Solid Films*, 2019, **679**, P. 79–85.

[9] Hamza Taha M.K., et al. Control of the compensating defects in Al-doped and Ga-doped ZnO nanocrystals for MIR plasmonics. *RSC Adv.*, 2017, **7** (46), P. 28677–28683.

[10] Sett D., Basak D. Toward understanding the role of VZn defect on the photoconductivity of surface-passivated ZnO NRs. *J. Phys. Chem. C*, 2017, **121** (44), P. 24495–24504.

[11] Ghosh S., Mallick A., et al. A novel blanket annealing process to achieve highly transparent and conducting Al doped ZnO thin films: Its mechanism and application in perovskite solar cells. *Sol. Energy*, 2018, **174**, P. 815–825.

[12] Varghese J., Vinodkumar R. Effect of CuO on the photoluminescence quenching and photocatalytic activity of ZnO multilayered thin films prepared by sol-gel spin coating technique. *Mater. Res. Express*, 2019, **6** (10), P. 1–27.

[13] Pearton S.J., et al. Transition Metal Doped ZnO for Spintronics. *MRS Proceedings*, 2007, **999**, 0999-K03-04.

[14] Silambarasan M., Saravanan S., Soga T. Mn-doped ZnO nanoparticles prepared by solution combustion method. *E-Journal of Surface Science and Nanotechnology*, 2014, **12**, P. 283–288.

[15] Sajjad M., Ullah I., et al. Structural and optical properties of pure and copper doped zinc oxide nanoparticles. *Results Phys.*, 2018, **9**, P. 1301–1309.

[16] Sato-Berrú R.Y., Vázquez-Olmos A., Fernández-Osorio A.L., Sotres-Martnez S. Micro-Raman investigation of transition-metal-doped ZnO nanoparticles. *J. Raman Spectrosc.*, 2007, **38**, P. 1073–1076.

[17] Bhattacharyya P., Basu P.K., et al. Noble metal catalytic contacts to solgel nanocrystalline zinc oxide thin films for sensing methane. *Sensors Actuators B*, 2008, **129** (2), P. 551–557.

[18] Wu L., Wu Y., Lü W. Preparation of ZnO Nanorods and optical characterizations. *Phys. E Low-Dimensional Syst. Nanostructures*, 2005, **28** (1)m P. 76–82.

[19] Habeebullah A., Alabi A.B., et al. Synthesis and Characterization of a dual-doped Zinc Oxide [(Na,N):ZnO] Nanoparticles by Wet Chemical Method. *African Review of Physics*, 2018, **13** (5), P. 29–38.

[20] Petersen D.H., Hansen O., Lin R., Nielsen P.F. Micro-four-point probe Hall effect measurement method. *J. Appl. Phys.*, 2008, **104** (1), 0137110.

[21] Moulzolf S.C., Frankel D.J., Lad R.J. In situ four-point conductivity and Hall effect apparatus for vacuum and controlled atmosphere measurements of thin film materials. *Rev. Sci. Instrum.*, 2002, **73** (6), P. 2325–2330.

[22] Bhosle V., Tiwari A., Narayan J. Electrical properties of transparent and conducting Ga doped ZnO. *J. Appl. Phys.*, 2006, **100** (3), 033713.

[23] Postica V., et al. Multifunctional Materials: A Case Study of the Effects of Metal Doping on ZnO Tetrapods with Bismuth and Tin Oxides. *Adv. Funct. Mater.*, 2017, **27**, P. 1–15.

[24] Tiginyanu I., et al. Strong light scattering and broadband (UV to IR) photoabsorption in stretchable 3D hybrid architectures based on Aerographite decorated by ZnO nanocrystallites. *Sci. Rep.*, 2016, **6** (1), P. 1–11.

[25] Shukla V.J., Patel A.J. Influence of Multiple Layers on Chemical Bath Deposited Zno Thin Films. *Int. J. Res. Appl. Sci. Eng. Technol.*, 2018, **6** (3), P. 268–274.
[26] Gayen R.N., Sarkar K., et al. ZnO films prepared by modified sol-gel technique. *Indian Journal of Pure & Applied Physics*, 2011, **49**, P. 470–477.
[27] Zhou H., et al. Raman studies of ZnO: Co thin films. *Physica Status Solidi (A) Applications and Materials Science*, 2007, **204** (1), P. 112–117.
[28] Liu X., Afzaal M., et al. Conducting ZnO thin films with an unusual morphology: Large flat microcrystals with (0 0 0 1) facets perpendicular to the plane by chemical bath deposition. *Materials Chemistry and Physics*, 2011, **127**, P. 174–178.
[29] Livneh T., Sterer E. Effect of Pressure on the Resonant Multiphonon Raman Scattering in UO2. *Phys. Rev. B: Condens. Matter Mater. Phys.*, 2006, **73**, 085118.
[30] Singh A.K., Viswanath V., Janu V.C. Synthesis, effect of capping agents, structural, optical and photoluminescence properties of ZnO nanoparticles. *Journal of Luminescence*, 2009, **129** (8), P. 874–878.
[31] Dingle R. Luminescent Transitions Associated With Divalent Copper Impurities and the Green Emission from Semiconducting Zinc Oxide. *Phys. Rev. Lett.*, 1969, **23** (11), P. 579–581.
[32] Garces N.Y., et al. Role of copper in the green luminescence from ZnO crystals. *Appl. Phys. Lett.*, 2002, **81** (4), P. 622–624.
[33] Peryakov D.S., Rembeza S.I., Menshikova T.G., Palkovnikov V.E. Influence of Annealing on the Electrophysical Properties of Copper Oxide (II) Thin Film, Prepared by Sol-Gel Method. *Nano Hybrids and Composites*, 2020, **28**, P. 48–52.
[34] Kumar R., Khare N. Temperature dependence of conduction mechanism of ZnO and Co-doped ZnO thin films. *Thin Solid Films*, 2008, **516** (6), P. 1302–1307.
[35] Park C.H., Zhang S.B., Wei S.H. Origin of p-type doping difficulty in ZnO: The impurity perspective. *Phys. Rev. B: Condens. Matter Mater. Phys.*, 2002, **66**, 073202.
[36] Rauch C., Gehlhoff W., et al. Lithium related deep and shallow acceptors in Li-doped ZnO nanocrystals. *J. Appl. Phys.*, 2010, **107**, 024311.